NOVA SCIENCE PUBLISHERS, INC.

METHODS AND MODELS TO DETERMINE THE GROUNDWATER FLOW IN ROCK MASSES: REVIEW AND EXAMPLES

LAURA SCESI
PAOLA GATTINONI

400 Oser Avenue, Suite 1600
Hauppauge, N. Y. 11788-3619
Phone (631) 231-7269
Fax (631) 231-8175
E-mail: main@novapublishers.com
www.novapublishers.com

ISBN: 978-1-61942-690-0 2012

ENVIRONMENTAL SCIENCE, ENGINEERING AND TECHNOLOGY

METHODS AND MODELS TO DETERMINE THE GROUNDWATER FLOW IN ROCK MASSES: REVIEW AND EXAMPLES

ENVIRONMENTAL SCIENCE, ENGINEERING AND TECHNOLOGY

Additional E-books in this series can be found on Nova's website under the E-book tab.

ENVIRONMENTAL SCIENCE, ENGINEERING AND TECHNOLOGY

METHODS AND MODELS TO DETERMINE THE GROUNDWATER FLOW IN ROCK MASSES: REVIEW AND EXAMPLES

LAURA SCESI

AND

PAOLA GATTINONI

Nova Science Publishers, Inc.

New York

For permission to use material from this book please contact us:
Telephone 631-231-7269; Fax 631-231-8175
Web Site: http://www.novapublishers.com

LIBRARY OF CONGRESS CATALOGING-IN-PUBLICATION DATA

ISBN: 978-1-61942-690-0

Published by Nova Science Publishers, Inc. † New York

CONTENTS

Preface		**vii**
Chapter 1	Introduction	**1**
Chapter 2	The Conceptual Model of Rock Masses	**3**
Chapter 3	Main Flow Direction in Non Saturated Rock Masses	**11**
Chapter 4	Groundwater Flow in Satured Rock Masses	**21**
References		**43**
Index		**51**

PREFACE

Water circulation in rocks is a very important element in the solution of quite typical problems arising in environmental, civil and mining engineering. Still, aquifers in rocks are devoted much less attention than those in porous media, partly because they are considered less important from the point of view of water research, and partly because rock masses are a very complex medium, (heterogeneous, anisotropous and discontinuous), therefore its modelization is quite complex. This paper proposes a review of the methodologies used for groundawater flow reconstruction in jointed rock masses (mainly based on the recent book written by Scesi and Gattinoni, 2009), describing the most recent researches concerning groundwater flow in rock masses through applicative examples. In particular, the identification of the main flow direction is very important to evaluate the groundwater flowing in the system, still this kind of analysis requires an accurate reconstruction of the hydrogeological conceptual model and a following critical choice of the most suitable modeling approach.

Chapter 1

INTRODUCTION

Water circulation in rocks occurs through a system of “vacuums” that is quite different from that of soils in dimensions, shape and density. The “vacuums” present in rocks can be divided in two wide categories:

- vacuums due to lack of cementation, degassing, dishomogeneous consolidation of the rock mass, dissolution of rock portions, etc.
- vacuums generated by cooling phenomena, stratification, schistosity, fractures and faults of tectonic origins, karsts phenomena, etc.

In the first case, the rock is divided in small fragments, similar to granules of soil; therefore, if there vacuums are interconnected, the water flow patterns are similar to those in porous media. In the second case, the cracks network (discontinuities) divides the rock in quite big portions and the water flow results strongly influenced by the geometric and mechanical characteristics of those vacuums. Therefore, a distinction has to be made between: intact rock, element constituted by granules or crystals, bound by permanent cohesive forces (with no discontinuities), and rock mass, physical body constituted by blocks of intact rock separated by discontinuities. Intact rock is a continuous medium with almost no permeability and porosity, whereas rock mass is a non continuous medium where discontinuities determine the hydraulic behaviours of the whole.

Therefore, knowing the origin, features and distribution of those vacuums is fundamental to better understand how water flows in rocks and therefore to reconstruct a representative hydrogeological conceptual model. This report intends to review and synthesize some researches on the topic of water flow in rock masses and it is manly based on the recent book by Scesi and Gattinoni (2009). In particular, the definition of the conceptual model is widely discussed, as it is fundamental for the identification of the main flow direction and the following choice of the modeling approach, both in satured and in non satured conditions. For the latter case, after a discussion of the main theoretic aspect, an example of water inflow in underground mines is proposed, showing the influence of the geo-structural setting on the percolation processes. Afterwards, the different modeling approaches are discussed, both from a theoretical point of view and with applicative examples, showing the main differences among continuum, discrete and combined approaches.

Chapter 2

THE CONCEPTUAL MODEL OF ROCK MASSES

Aquifers, and aquifers in rock masses in particular, present a relevant heterogeneity in the study scale used to solve application problems (slope stability, road and tunnel construction, etc.). The presence of those heterogeneous features, often combined with a marked anisotropy of the medium, implies the need of a careful reconstruction of the hydrogeological structure, so as to make the conceptual model acceptable and the forecast of the water flow reliable enough; usually, the waterflow is ruled by the orientation and the hydraulic features of the joints. Therefore, for the conceptual model definition it is fundamental to carry out a geological-structural and a geological-technical study to highlight the main parameters and the main features of discontinuities (Table 2.1). The most important features of discontinuities are:

- *Orientation:* in rocks with fissural or fracture permeability, water flows along confined paths, thus determining a marked orientation of the water flow. As a consequence, it is evident that the discontinuities orientation strongly influences the flow direction. In any case, the real flow of the groundwater is diverted by the walls delimiting the discontinuities and liquid particles are bound to follow a longer path.
- *Fracturing degree:* quantity and proximity of fractures pervading a rock mass define the fracturing degree of the rock and, as a consequence, its permeability. Spacing, intercept,

frequency, RQD coefficient (Rock Quality Designation) and Unitary Rock Volume (URV) are the features that allow the description of the fracturing degree of a rock mass. From the hydraulic point of view, a low value of spacing or intercept and, as a consequence, a high value of frequency favour underground water circulation, as they indicate a marked fracturing of the rock; and the smaller the dimensions of unitary block, the bigger the quantity of water that can percolate.

- *Persistence:* is defined as the extension of a discontinuity with respect to a reference line belonging to the plane on which the discontinuity lies (expressed as a percentage). Generally, if persistence is over 80% the hydraulic behaviour of the rock mass is basically conditioned by water flow inside discontinuities; while, if persistence is less than 25%, water flow is almost hindered due to the lack of interconnections among different discontinuities, that therefore create isolated and localized zones where water flows.
- *Aperture and Filling:* the aperture of a discontinuity represents the distance between the discontinuity walls. Outcropping apertures can be influenced by external factors, such as stress loosening and superficial weathering, and they are usually wider than those present inside the rock mass. The presence of filling in discontinuities must be recorded considering its width, mineralogical composition (calcite, silt, clay, sand, etc.), grains size distribution and moisture conditions.
- *Roughness:* discontinuity surfaces can be planar, undulating, stepped or irregular. Roughness is the mean height of asperities of the surface relative to the mean aperture. From the hydraulic point of view, roughness reduces the effective aperture of discontinuities and its influence increases as the aperture gets smaller (Bandis et al., 1985; Scesi and Gattinoni, 2007). Various studies were carried out measuring how roughness and fracture apertures variations affect water flow; they highlighted that roughness and undulations of the discontinuities walls determine points of contacts and rock bridges that can be modelled through various statistical distributions of joints apertures. In the presence of rough joints, also the application of a load can affect considerably the permeability values of the joint; actually,

dilatancy phenomena determine variations of the hydraulic aperture of the joints that are strictly correlated to those of mechanic aperture.

- *Weathering:* the weathering process determines an increase of porosity and therefore a higher propensity of the rock to let water pass through; exceptions are represented by those cases where the weathering process leads to the formation of levels and clayey filling characterized by very low permeability.

Table 2.1. Surveys and Analysis for the Hydrogeological Characterization of Rock Masses at Different Scales

Characterizing factors	Surveys and analysis	
	Large scale	Local scale
Joints	Photointerpretation for master joints orientation Laserscanning for frequency and persistence	In situ geologicial-structural survey (orientation, spacing, aperture, persistence, roughness, etc.)
Water table and gradient	Resurgence points (i.e., springs)	Piezometers
Hydraulic conductivity	Hydrogeochemical survey (e.g., tracer tests or depletion function of springs)	Structural data elaboration (for surface level) In bore-hole tests (for in depth evaluation)

Based on the features of the joints previously described (mainly on fracturing degree and persistence), three main kinds of flow network can be identified (Fig. 2.1):

- Dominant drain: the rock mass is characterized by a low fracturing degree and a main joint set rules the groundwater flow, whereas the other minor joint sets have low persistence and do not contribute to the flow; in this case, main flow paths exists in the rock mass,
- Multiple drains: there exist two or three well developed joint sets, having a good persistence and connectivity; therefore, the groundwater flow takes place in a wide and articulated network of fractures,
- Dispersive structure: in the rock mass no main flow path exits, as the rock mass is characterized by a high fracturing degree with several persistent and well interconnected joint sets.

In the first case the flow is certainly ruled by the joints features, whereas in the third one the rock mass can be studied as a continuum. The second case can be assimilated to both a discrete network and a continuum. In particular in this case, based on the work scale and the data availability, the definition of the hydrogeological conceptual model has to better consider the following aspects:

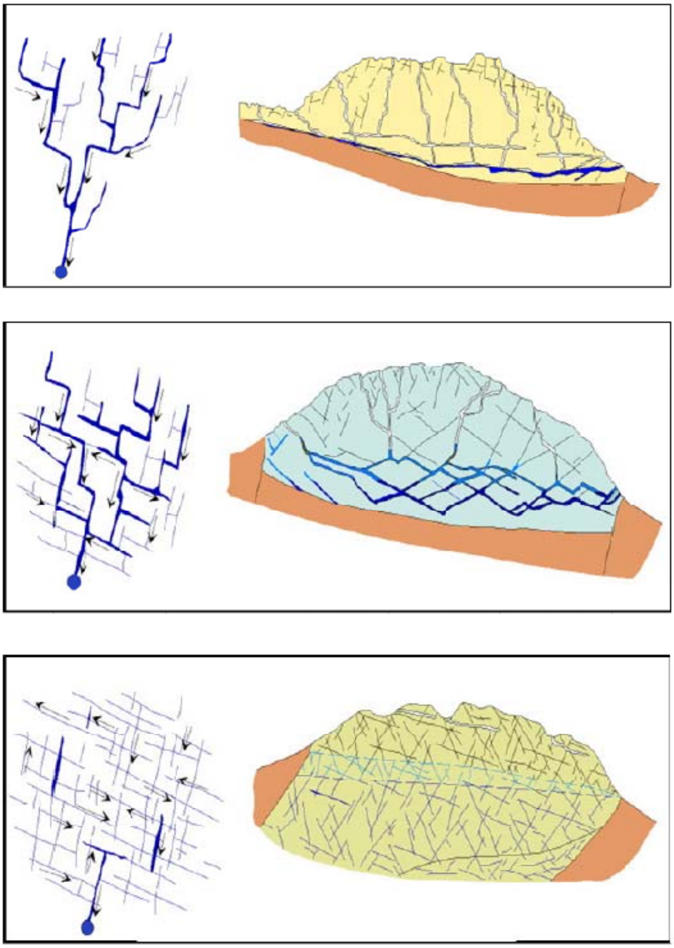

Figure 2.1. Flow network typology in rock masses: (a) dominant drain, (b) multiple drains, (c) dispersive (Civita 2005).

- the work scale (Bear and Berkowitz, 1987);
- the fracturing degree (in term of the elementary representative volume);
- the changing of fracturing degree in the space, in particular with depth.

As regard the work scale, in a near and very near field the water flow generally occurs inside a single fracture or in a small number of well defined fractures, whose shapes and position are known, and that may also be reconstructed with a statistical approach (Dershowitz and Einstein, 1988; Meyer and Einstein, 2002; Min et al., 2004 and references therein). For problems on lower scales (far and very far field) continuous approaches are generally required. Obviously the choice depends not only on the work scale, but also on the fracturing degree of the rock mass (La Poine et al., 1996) that define the Representative Elementary Volume (REV). This latter is the minimal volume to take into consideration to study the hydrogeological features of a rock, such that the medium can be considered sufficiently homogeneous and isotropic (Bear, 1972). In a rock mass, the REV must contain all the different discontinuity families and therefore it can change, according to the fracturing degree, from 1 m^3 to 106 m^3.

In addition to the work scale and the fracturing degree, in the conceptual model definition it has to be taken into account that generally experimental observations show a reduction of the frequency of fracturing as depth increases, linked with a reduction of the aperture of joints (Snow, 1969). This determines an often quite relevant decline of the effective fracture porosity with depth, with a correlated decline of the permeability. In reality, the definition of the trends in depth of the above mentioned geometric features of discontinuities is often quite difficult and experimental tests carried out by different Authors during the years have often provided contrasting results. According to some Authors, for examples, beyond a superficial unit of weathered rock, where the fracturing frequency is higher, permeability remains almost constant in depth (Raven and Gale, 1976; Kendorski and Mahtab, 1976; Manev and Avramova-Tacheva, 1970); permeability changes should therefore be linked to aperture changes more than to variations in the intensity of fracturing, even though the presence of wide open joints in depth is not uncommon, with extremely variable permeability values that could not be easily reproduced by means of empirical laws, in particular when depth exceeds 500 m (Brace, 1980).

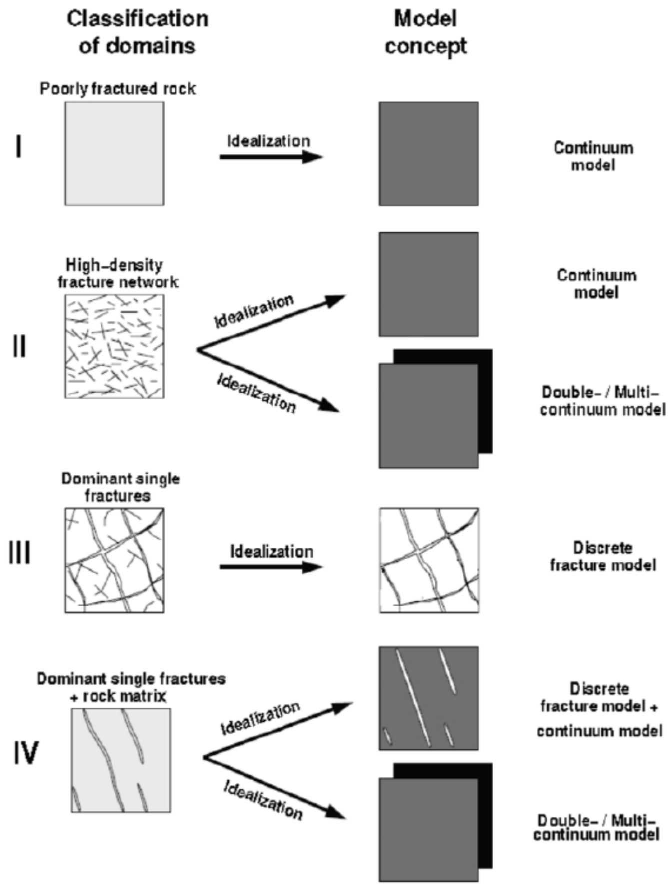

Figure 2.2. Classification domains and the corresponding conceptual models (Dietrich et al., 2005).

On the basis of the previously described information for modelling purpose, the rock mass domains can be classified as (Fig. 2.2):

- Poorly fractured rock: the corresponding conceptual model is a continuum model, in which an equivalent hydraulic conductivity or the corresponding tensor have to be defined for the different homogenous zones;

- High-density fracture network: it can be idealize as both a single continuum or a double continuum, according to data availability;
- Dominant single fractures: the corresponding conceptual model is a discrete fracture model, in which joints features and distribution have to be well known;
- Dominant single fractures in addition to rock matrix: it can be idealize as both a double continuum model or a combination of continuum and discrete fracture model; in the latter case, characterization of both continuum and joints features are need, in addition to an exchange function.

Chapter 3

MAIN FLOW DIRECTION IN NON SATURATED ROCK MASSES

This section analyzes the waterflow conditions inside rock media in non-saturated (percolation flow) conditions, and it presents an easy to apply procedure to determine the main flow direction. In particular, starting from the structural discontinuity features, it is possible to determine the main percolation direction, also as a function of the joints interconnectivity. Moreover, this information can be plotted using stereographic representations.

3.1. THEORETIC ASPECTS

To determine the main flow direction in a fractured medium it is important to take following elements into consideration:

- the permeability of single discontinuity set,
- the orientation of each set,
- the interconnection among the sets,
- the flow conditions (i.e. non-saturated),

In a non-saturated rock mass, the water flow inside discontinuities is ruled by gravity, therefore water tends to flow in depth following the orientation of discontinuities, especially the ones with high hydraulic conductivity. The water percolation goes on till it reaches either a watertable (in that case, a flowing condition occurs in the saturated medium that is ruled by the hydraulic gradient of the aquifer) or an impermeable layer that acts as a bedrock. Therefore, the flow directions during the percolation phase coincide with the dip direction of each discontinuity family. The main flow direction is calculated by combining the discontinuity orientations, also considering the above mentioned flow components along the discontinuity sets (Table 3.1 and Fig. 3.1a).

Table 3.1. Discontinuity sets considered in the example

Discontinuity sets	Dip Direction and Dip	Aperture (m)	Frequency (1/m)	Hydraulic conductivity (m/s)
F_1	90°/65°	0.00126	0.1	1.635E-04
F_2	300°/30°	0.001	0.1	8.175E-05
F_3	240°/50°	0.001	0.1	8.175E-05

In the example of Table 3.1 the main flow direction has the following dip direction and dip: 284°/81°. On the contrary, if the apertures of the different joint sets are equals, the main flow direction has the following dip direction and dip: 277°/68°. The structural diagram in Figure 3.1b shows the stereographic representation of each percolation direction and the main flow direction resulting from them.

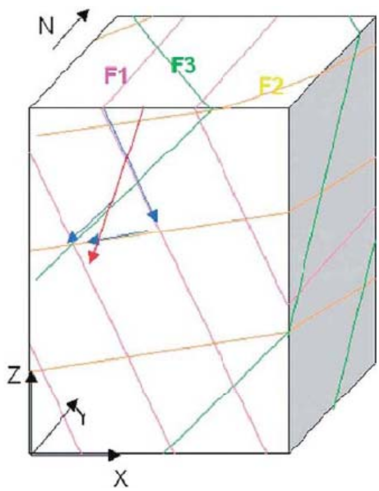

a

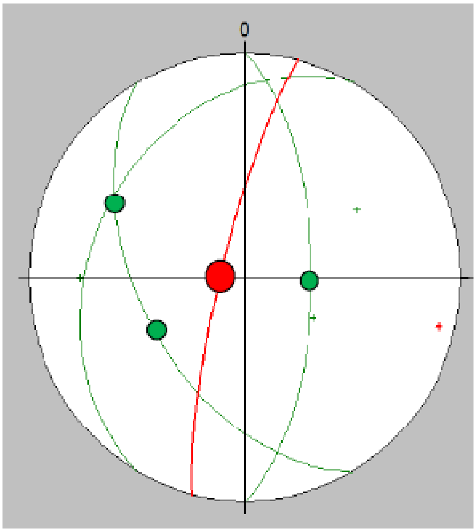

b

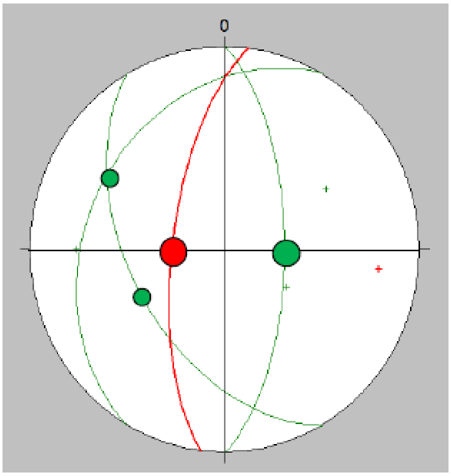

c

Figure 3.1. (a)Tridimensional view of the discontinuity sets associated to the three main percolation direction (in blue) and of the main flow direction (in red). Stereographic representation of the main flow direction in a non-saturated medium: (b) the apertures are not equals, (c) the apertures are equals: the size of colored circles, representative of hydraulic conductivity vectors, is proportional to the modulus of hydraulic conductivity itself.

A further aspect to consider to reconstruct the preferential flow direction of the flow is the degree of interconnection among the different discontinuities; actually, if fractures are independent from each other, they behave as isolated bonds that do not contribute to the shift of the fluid mass. If, on the contrary, the discontinuities are interconnected, hydraulic conductivity is influenced by all discontinuity families present in the rock mass and the water flow follows a real flow network formed by a series of bonds connected to each other (fig. 3.2).

Rouleau and Gale (1985) proved that interconnection (I_{ij}) between two discontinuity families may be expressed as a function of other parameters characteristic of the same discontinuity families, such as orientation, spacing and persistence:

$$I_{ij} = \frac{l_i}{s_i} \sin \gamma_{iJ} \quad i \neq j \tag{1}$$

where l_i e s_i are respectively the length and the average spacing of the ith discontinuity family, whereas γ_{ij} is the angle between the two discontinuity families. In general, it happens that:

$$I_{ij} = I_{ji}$$

If n represents the number of discontinuity families inside the rock mass, the comprehensive interconnection of the ith discontinuity family is given by:

$$I_i = \sum_{j=1}^{n} I_{ij} \quad i \neq j \tag{2}$$

Naturally, when I_i increases, the load of the ith discontinuity family increases from the hydraulic point of view. The unit is assumed as the limit value of the interconnection index I_i:

if $I_i > 1$, the i^{th} discontinuity family is interconnected with the rest of the discontinuous system;

if $I_i < 1$, the i^{th} discontinuity family is isolated from the rest of the discontinuous system.

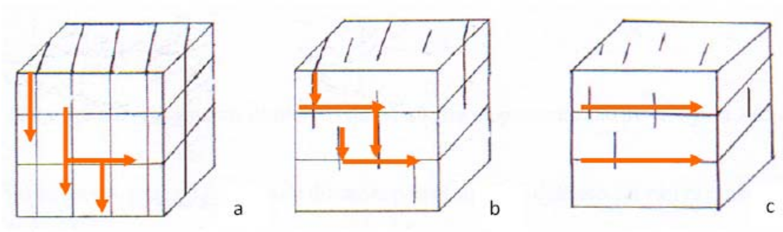

Figure 3.2. Tridimensional representation of fracture systems with different interconnectivity degree: (a) completely interconnected, (b) partially interconnected, (c) not interconnected.

3.2. Non Satured Medium: The example of the "Fontane Mine" (Salza di Pinerolo – Turin, Italy)

In the municipality of Salza di Pinerolo (Val Germanasca-Turin-Italy, Fig. 3.3) there is an important talc mine called "Fontane Mine ". It is an underground mine, which is spread over many levels. In particular, in the section named Gianna, there are seven unused levels, connected by shafts, and an eighth level, now active, known as "Section Rodoretto". The study included two levels (Fig. 3.4) still available, used as a museum: the Paola level (1,212 m a.s.l.) and the Gianna level (1,265 m a.s.l.).

Figure 3.3. The red star represents the study area (Germanasca Valley. Turin, Italy).

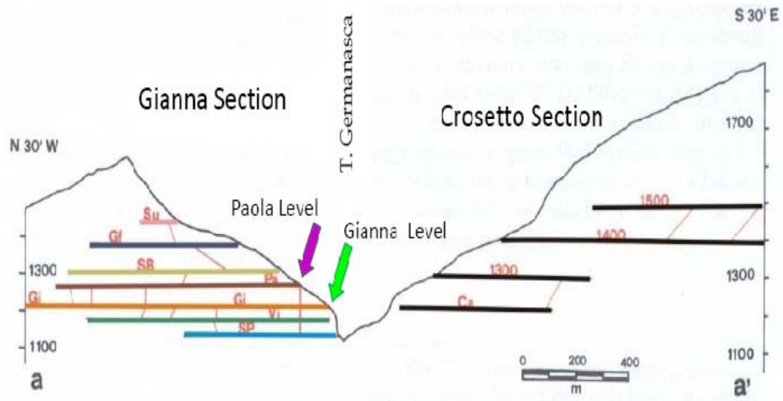

Figure 3.4. Cross section of the “Fontane mine” The arrows show the two studied levels: Paola Level (in violet) and Gianna Level (in green).

The geological survey, carried out within the two considered tunnels, allowed to recognize, from North to South, the following lithologies (Fig. 3.5):

- Paola Level: gneiss (for about 400m), micaschists and gneiss interspersed with marbles (for 280m) and micaschists (for 680m);
- Gianna Level: micaschists (190m), gneiss (70m), micaschists and marbles (415m), micaschists (700m).

Within the same tunnels, the structural survey has revealed the presence of a large number of faults and discontinuity families, in particular the following alignments were recognized (Fig. 3.6):

- normal faults trending ENE-WSW;
- reverse faults trending NNE-SSW and E-W;
- faults trending NW-SE and NNW-SSE, which represent the reactivation of the schistosity;
- discontinuity Systems F1 (having dip direction to North or to South and average dip close to vertical) and F2 (corresponding to the regional schistosity).

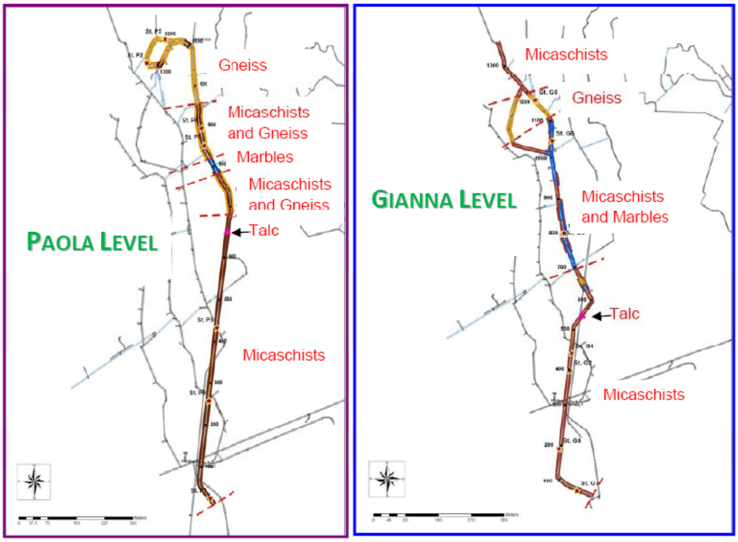

Figure 3.5. Lithologies recognized inside the two studied levels (Paola and Gianna).

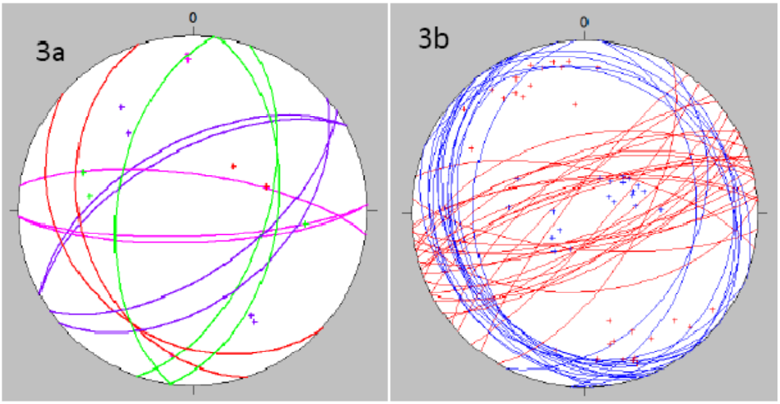

Figure 3.6. The most important fault systems (a) and discontinuity families (b) surveyed inside the two studied mines.

The two levels Paola and Gianna were divided into different stretches depending on the presence or absence of water. The analysis of the dripping from the discontinuities allowed to conclude that they are continuous and also visible in the dry season, while the humidity level inside the tunnels, more pronounced near the openings, changes seasonally.

The surveys carried out and the results obtained from the electrical tomography, allowed to exclude the presence of groundwater levels in the two tunnels Paola and Gianna, which are thus in non-saturation condition.

In light of these considerations, it was possible to determine:

- the main flow directions: in the unsaturated medium the water flow directions coincide with the dip direction of each discontinuity families. So to determine the main percolation direction is necessary to combine the components of motion along all the discontinuity sets;
- the tunnel inflow: expressed as a function of the intersection probability between the tunnels and the discontinuity families, this probability depends, in turn, by the orientation of discontinuities and tunnels, spacing and persistence of the discontinuities and length and diameter of the tunnels.

The tunnel inflow were calculated for each stretch lithologically homogeneous, through the following relationship (Scesi and Gattinoni, 2009):

$$Q = \sum_i k_i \frac{2rL \sin a_i^{app}}{\lambda_i \cos \beta_i} e_i \tag{3}$$

where:

k_i = permeability of the i^{th} discontinuity family (m/s)

r = radius of the tunnel (m)

e_i = average aperture of the i^{th} discontinuity family (m)

α^{app} = apparent dip of the i^{th} discontinuity family in the tunnel direction (°)

λ_i = spacing of the i^{th} discontinuity family (m)

β_i = angle between dip direction of the discontinuity and tunnel direction

L = length of tunnel (m)

The performed calculations allowed to obtain the following results: along the Paola level the total flow rates were equal to 0.43l/s (Table 3.2), while along the level Gianna the total flow rates were equal to 4.42 l/s (Table 3.3).

Table 3.2. Paola Level: Flow rates [l/s] calculated in the different stretches

Stretch	1	2	3
Lithology	Gneiss	Contact Micaschists - Gneiss	Micaschists
Length [m]	400	280	680
Flow rate [l/s]	0.01	0.10	0.32

Table 3.3. Gianna Level: Flow rates [l/s] calculated in the different stretches

Stretch	1	2	3	4
Lithology	Micaschists	Gneiss	Contact Micaschists - Marbles	Micaschists
Lunghezza [m]	190	70	415	700
Flow rate [l/s]	0.15	0.60	3.66	0.01

In order to validate the model, in addition to the census of water inflows, a monitoring survey was carried out, through the placement of spillways.

In Figure 3.7 it is possible to see the obtained results, compared with the tunnel inflow previously analytically calculated.

The Figure 3.7 shows that the tunnel inflow values obtained analytically vary little from those measured in situ, confirming that structural methods can represent a useful tool in the determination of hydrogeological parameters.

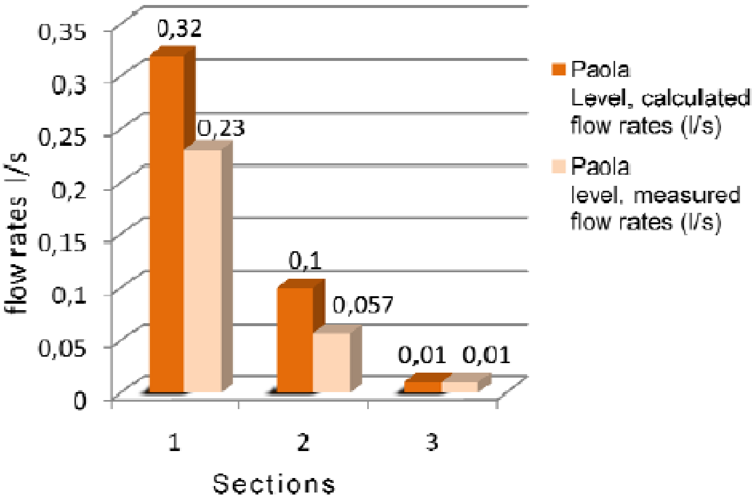

(a)

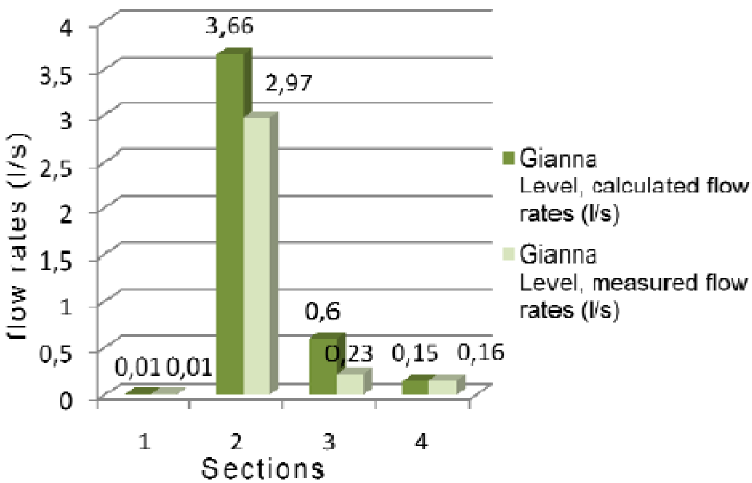

(b)

Figure 3.7. Comparison between the measured and calculated flow rates inside the Paola (a) and Gianna (b) levels for every considered section.

Chapter 4

GROUNDWATER FLOW IN SATURED ROCK MASSES

In satured rocks with fissural or fracture permeability, water flows according to the hydraulic gradient but along confined paths, determined by discontinuity orientation (Fig. 4.1). As a consequence, it is evident that the discontinuities orientation strongly influences the flow direction.

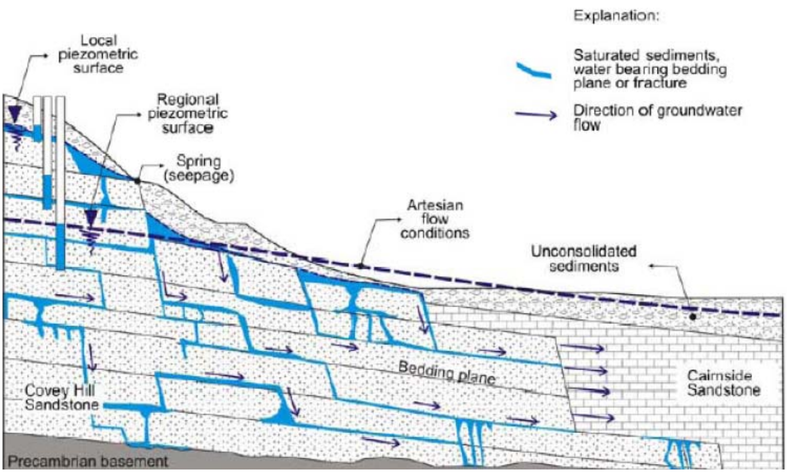

Figure 4.1. Conceptual model of a rock mass aquifer with groundwater flow direction (Nastev et al., 2008).

More in detail, at small scale (domain dimension < REV, Fig. 4.2a), the water flow in satured rock masses is ruled by the hydraulic conductivity of the fractures, whereas at large scale (domain dimension > REV, Fig. 4.2a) the rock mass can be assimilate to an anisotropic continuum and the tensor of the hydraulic conductivity can be considered in the groundwater flow reconstruction. In some cases, a REV cannot be defined, so that the rock mass has to be modelled as a discrete fracture network at all scale of analysis (Fig. 4.2b).

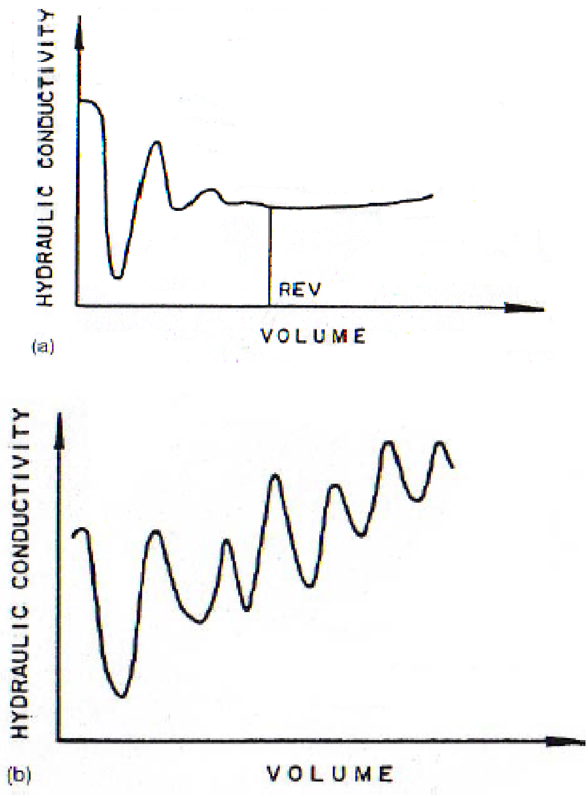

Figure 4.2. Hydraulic conductivity trend with volume support dimension: (a) for volume of support dimension < REV the groundwater flow is controlled by fractures, whereas for dimension > REV a continuum approach is possible; (b) no REV con be defined and therefore the groundwater flow is always controlled by fractures (Lee and Farmer, 1993).

As far as groundwater flow simulation is concerned, numerical models are became in the last decades very useful tools, in which the fundamental flow equations are solved on the basis of known boundary and initial conditions. Obviously, the first step of the modelling procedure, after the conceptual model definition, is the choice of the general equation describing the phenomena, i.e., the choice of the modelling approach.

4.1. THE CHOICE OF THE MODELING APPROACH

Different models are available to reconstruct the groundwater flow in saturated rock masses, spanning from continuum approaches (single, double or multiple) to discrete models through combined approaches (Fig. 4.3). The choice of the most suitable model in a specific case study depends on the previously defined conceptual models. The choice whether to use the one or the other method is made also on the basis of the available geological-structural data and the work scale. It is important to underline that the results provided by numerical modelling may contain errors linked both to the limited ability of the model itself to represent the real geological structure and to the difficulty of characterizing the discontinuity network in the scale required.

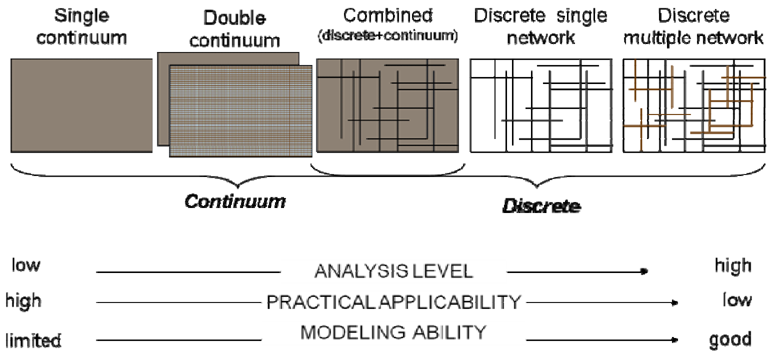

Figure 4.3. Scheme of the different modeling approaches.

4.1.1. Continuum Models

Many authors use Darcy's models for the schematization of fracture systems, making references to the concepts of equivalent hydraulic conductivity and Representative Elementary Volume. Evidently, that is possible only when a REV can be set within the domain to be studied (Fig. 4.2). Generally, the continuum choice occurs according to the knowledge on the distribution of fractures and hydraulic conductivity and according to the computational time required by the elaboration. Models based on the use of the equivalent continuum solve the fundamental equation of flow in porous media:

$$k_x \frac{\delta^2 h}{\delta x^2} + k_y \frac{\delta^2 h}{\delta y^2} + k_z \frac{\delta^2 h}{\delta z^2} = \frac{1}{1+e}\left(e \frac{\delta S}{\delta t} + S \frac{\delta e}{\delta t}\right) \tag{4}$$

where k_i are the hydraulic conductivity components, e the porosity and S the saturation degree.

One of the most used numerical code is Modflow (Harbaugh et al., 2000), which solves the above mentioned flow equation in 3-D through a finite difference method at central cells. At this aim the domain is divided with a square or rectangular mesh, having cell of dimension higher then REV. As the presence of extended shear zones highly conditions the groundwater flow, the continuum models have to keep into account the presence of these structural features that represent basic elements in the ruling of groundwater flow. To solve the problem, boundary conditions have to be defined: constant head, constant flux or head depending on flux. Generally, the results obtained from the application of Darcy's models underline how strongly the model calibration is influenced by the dimension of the cells used and the availability of field measures (Fig. 4.4).

4.1.2. Discrete Models

The continuum approach is no longer valid if the system is studied on a detailed scale, as this scale requires discrete flow models. This implies the need to generate a discontinuity network and to apply the appropriate boundary conditions to it, in order to decide which are the most suitable numerical techniques for the flow forecast. Discrete models developed both in two dimensions (Long and Witherspoon, 1985; Robinson, 1982) and in a three-dimensional field (Hung and Evans, 1985; Rasmussen, 1988; Andersson and Dverstorp, 1987; Dverstorp and Andersson, 1989) explicitly simulate the flow of each single discontinuity using, for example, the Navier-Stokes equation (Bear, 1993), Kirchoff's laws for electric circuits (Kraemer and Haitjema, 1989) or the model with hydraulically connected circular disks (Cacas et al., 1990). Actually, also in the international literature, the application of models based on the flow hypothesis along discontinuities (Diodato, 1994) is either limited to simplified or limited cases (McCaffrey and Adinolfi, 2003; Jeong et al., 1999; Machado et al., 2001) or it is referred to very specific and detailed studies (Oxtobee and Novakowski, 2003). In that sector, the application of numerical models with distinct elements arises particular interest; they can analyze the groundwater flow both in a two-dimensional and a three-dimensional field. But such an approach requires the availability of rich quantities of data about the underground and, as a consequence, it was used more often for the study of tunnel inflows (Papini et al., 1994; Molinero et al., 2002). In order to provide satisfactory results, the discrete approach must include detailed information on the characteristics of the discontinuities. Therefore, it allows the simulation of local phenomena or detailed scale processes, whereas it is not suitable to model generic scale processes, due to the computational limitation linked to the large quantities of required data. Often, the discrete approach is appropriate when there are discontinuity systems of localized shear zones that are ruling the water flow (Samardzioska and Popov, 2005).

An example of a mathematical model that can simulate the groundwater flow within discontinuities, using a numerical methods with distinct elements, is the UDEC code (Universal Distinct Element Code, Itasca 2001). UDEC is a numerical program based on a distinct element method that simulates the response of discontinuous media subjected to static or dynamic loads, flows and thermal gradients. It is based on a Lagrangian calculation scheme, in which the rock mass is represented by a set of blocks interacting with each other only in the contact points; the behaviour of the whole is governed by the characteristics of the contacts (deformable or not deformable) and of blocks mechanical properties (rigid or deformable). To simulate the deformable nature of the contacts a system of springs (having a known stiffness both in the normal and in tangential direction) is interposed between the rigid blocks. UDEC assumes blocks to be impermeable and the groundwater flows only through fractures. The groundwater flow in a joint depends on its hydraulic aperture *a*, which is, in turn, affected by pore water pressure within the joint (hydro-mechanically coupled):

$$a = a_0 + u_n \tag{5}$$

where a_0 is the joint hydraulic aperture at zero normal stress (i.e. in the surface) and u_n the joint normal displacement. The algorithm matches the mechanical and hydraulic behaviour of the system: in fact, the aperture, and then the joints permeability, is related to the mechanical deformation, which, in turn, is influenced not only by the lithostatic load but also by water pressure in fractures. Generally, a minimum value a_{res} is assumed for the aperture, below which mechanical closure does not affect the joints permeability. The flow rate is calculated (for edge-edge contact) using the following cubic law:

$$q = -\frac{a^3}{12\mu} \cdot \frac{\Delta p}{l} \tag{6}$$

where μ is the dynamic water viscosity; *a* is the joint hydraulic aperture; *l* is the contact length; Δp is the pressure change along the contact.

In the UDEC code, also the joints persistence can be considered, controlled through the trace length of joint segment of the i^{-th} family l_i, and the gap length between joint segments (corresponding to the rock bridge length) of the same i^{-th} family g_i. Both the trace and the gap length can be defined in terms of mean geometric properties and standard deviation.

In this way, a mechanical-hydraulic study can be carried out, where the joint hydraulic conductivity also depends on the mechanical deformation that, in turn, is influenced by the water pressure inside the discontinuities (Fig. 4.5). That approach allows the reconstruction of the flow network inside the rock masses, thus determining both discharge and water pressures in single discontinuities, and it is particularly useful in the solution of problems regarding slope stability and the drawing of projects for underground works.

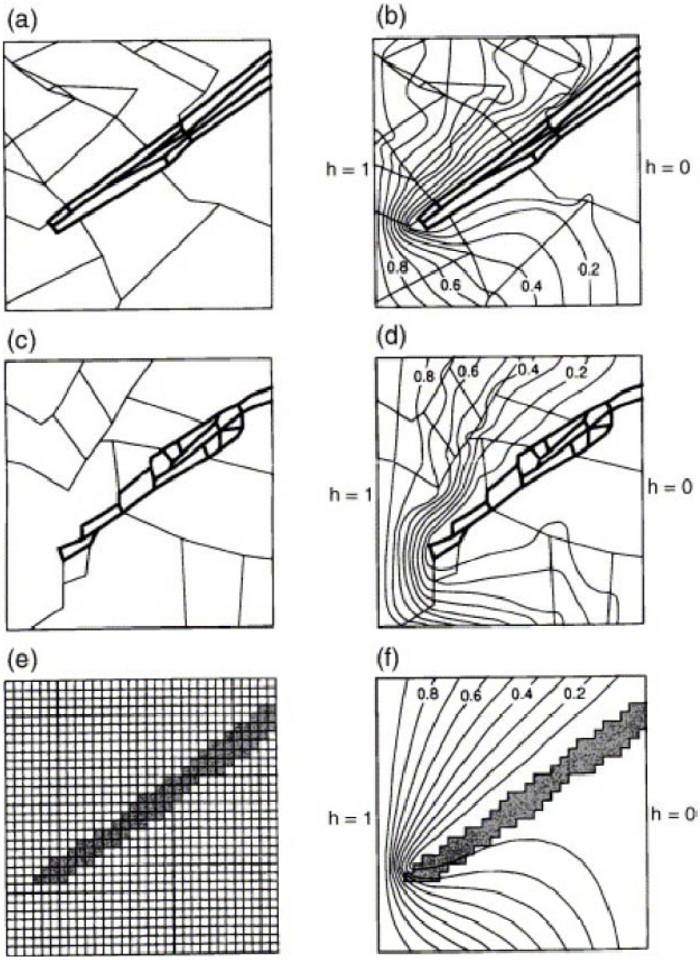

Figure 4.4. Illustration of fractured geological heterogeneity and its representation in numerical flow models: (a) real fracture network and (b) its distribution of head; (c) discrete fracture (DF) model and (d) corresponding distribution of head; (e) continuum model and (f) its corresponding distribution of head (Hsieh, 1998).

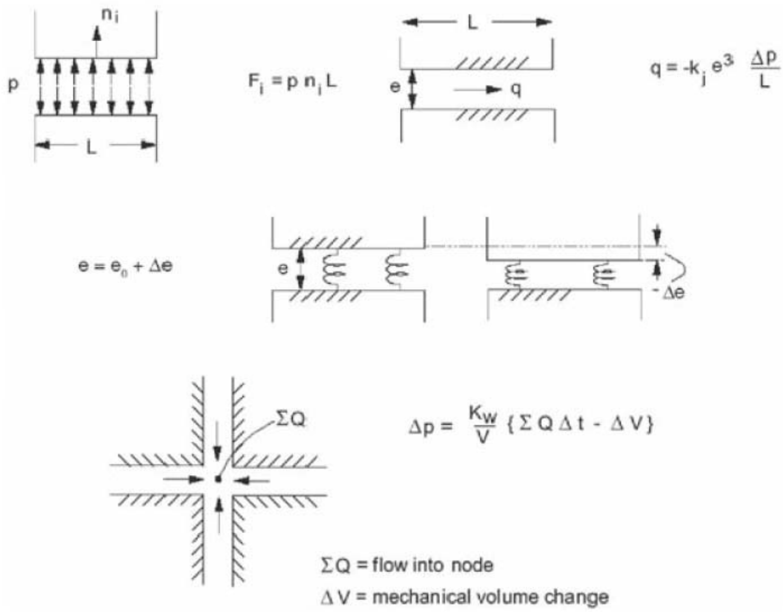

Figure 4.5. Schematization of the solid–fluid interaction within discontinuities: (a) Water pressure; (b) water discharge; (c) mechanical effects induced by stresses affecting the aperture; and (d) pressure change in the sites (Itasca, 1999).

4.1.3. Combined Approach: Dual Porosity and Dual Permeability Models

The discrete approach is originated from the observation that non-fractured rocks may present high porosity (storage coefficient) with very low hydraulic conductivity (lack of flow); on the contrary, high hydraulic conductivity (and therefore flows) can be present within fractures, even with small storage volumes. Dual porosity models (introduced by Barenblatt et al. in 1960 and then implemented by Warren and Root in 1963 and Kazemi in 1969) try to combine the simplification of Darcy’s models with the complexity of discrete models, taking into account, at the same time but still separating from one another, the water flow within intact rock (primary porosity) and that of the discontinuity network (secondary porosity). Actually, in dual porosity models, equations are used that can rule both continuous and fractured media, among which flow exchange at the interface is possible (Fig. 4.6). Some examples of semi-analytical and numerical models were proposed by Huyakorn et al. (1983), Rowe and Booker (1990) and Sudicky (1990). Generally, dual porosity models are used to simulate the flow and transportation of contaminants (Bai et al., 1997; Moutsopoulos et al., 2001; Alboin et al., 2002) as these elements may have relevant interaction with the rock matrix, mainly in relation to the propagation and dispersion of the contaminant. Some limitations of dual porosity models are represented by the little realistic adoption of a very simplified geometry of rock masses and by the fact that the advection in the rock matrix is generally neglected.

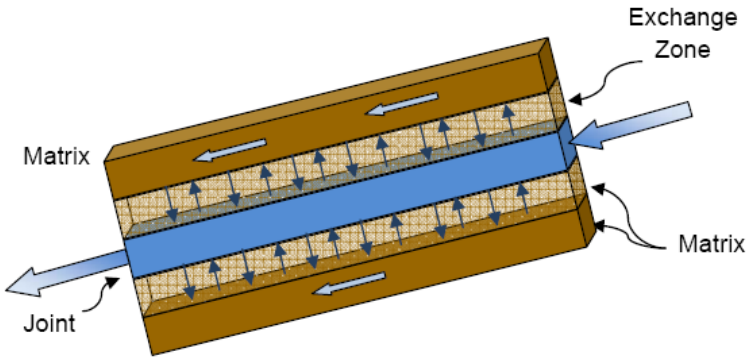

Figure 4.6. Flow exchange between rock matrix and fracture in combined approach. The light blue arrows inside the matrix indicate that the flow can also occur in the rocks (dual permeability).

Moreover, the delay in the hydraulic response of rock masses, well described by the dual porosity models as a consequence of the high storage coefficient of the rock matrix, is often influenced also by the presence of small but very frequent fractures in the rock matrix, especially in the nearby area of the master joints. Therefore, rock matrix achieves a not negligible permeability with the possibility of local flow and water exchanges with the master joints. In this case “double permeability models” can be more useful to better describe the phenomena (Clifford, 2001).

The equations to solve in one dimensional case are for dual permeability model:

$$S_1 \frac{\partial h_1}{\partial t} - T_1 \frac{\partial^2 h_1}{\partial x^2} = \kappa (h_2 - h_1)$$
$$S_2 \frac{\partial h_2}{\partial t} - T_2 \frac{\partial^2 h_2}{\partial x^2} = \kappa (h_1 - h_2) \qquad (7)$$

where h_1 and h_2 are the hydraulic heads of fractures and matrix respectively, S_1 and S_2 their specific storages, T_1 and T_2 their trasmissivities, and κ the exchange rate, depending on the specific exchange surface (i.e., the volume and geometry of matrix blocks), the discontinuity spacing, and the interface hydraulic conductivity. If the hydraulic conductivity of the rock matrix can be considered negligible with respect to the hydraulic conductivity of fractures, the above mentioned equations become:

$$S_1 \frac{\partial h_1}{\partial t} - T_1 \frac{\partial^2 h_1}{\partial x^2} = \kappa (h_2 - h_1)$$
$$S_2 \frac{\partial h_2}{\partial t} = \kappa (h_1 - h_2) \qquad (8)$$

In this latter case we speak of dual porosity models. Modflow 2005 introduces the possibility of using a combined approach with the Conduit Flow Process Packege, in which the exchange rate between rock matrix and fractures is calculated iteratively as a flux dependent on head, also considering through the Reynold's Number the possibility of turbulent regime within the fractures.

4.2. Example of Continuous Modeling Approach: The Nossana Spring

The example proposes a mathematical model aimed to simulate the groundwater flow in the fractured-karst media that forms the Nossana

Spring basin (Northern Italy) and, therefore, to understand the parameters which control the outflow from the spring in the depletion phase.

The recharge area of the Nossana Spring is located in the Central Prealpine Area (Bergamo District, Lombardy Region), and it covers an area of over 80 km^2 (Fig. 4.7). It is characterized by altitude ranging from 800 m a.s.l. to 2,500 m a.s.l. and it is made for the most part of carbonatic rocks (Chardon, 1975; Bini et al., 2000). As the Nossana Spring is the main outlet of the groundwater fed by this very wide basin, its discharge is quite high (on average 3 m^3/s). Furthermore, its regime is characterised by a considerable variability, having discharge ranging from 0.6 to 20 m^3/s. This great variability in the spring discharge is a typical characteristic of karstic catchment areas, such as in the case of the Nossana Spring, that is exactly the surface discharge point of a large fractured-karst aquifer (Jadoul et al., 1985). This aquifer develops in a large synclinal fold in the Triassic carbonate formation of the Esino Limestone, which is very permeable because of karstification, standing in tectonic contact on a marl formation (Fig. 4.7).

On the basis of the geological and hydrogeological characteristics of the area, the most important process components of groundwater flow model were identified and quantified (Fig. 4.8). The infiltration rate of the study area is actually very high and the water courses are mainly fed by groundwater, through the local quick draining and emptying out of the karst pipes and fractures present in the most superficial portion of the basin. Then, the recharge values were assessed on the basis of the available data of precipitation and temperature at different altitudes (Fig. 4.9), by calculating the evapotranspiration through the Thornthwaite formula. The surface hydraulic conductivity was assessed on the basis of the geo-structural setting and considering karst evidences. According to the in situ surveys, along the fractures a local increase of about one order of magnitude in the hydraulic conductivity was assumed for a 20 m wide strip. As the karst conduits in depth are mainly developed along fractures (Fig. 4.8), in the model they were considered like the fractures by introducing strips of high hydraulic conductivity both in surface and in depth.

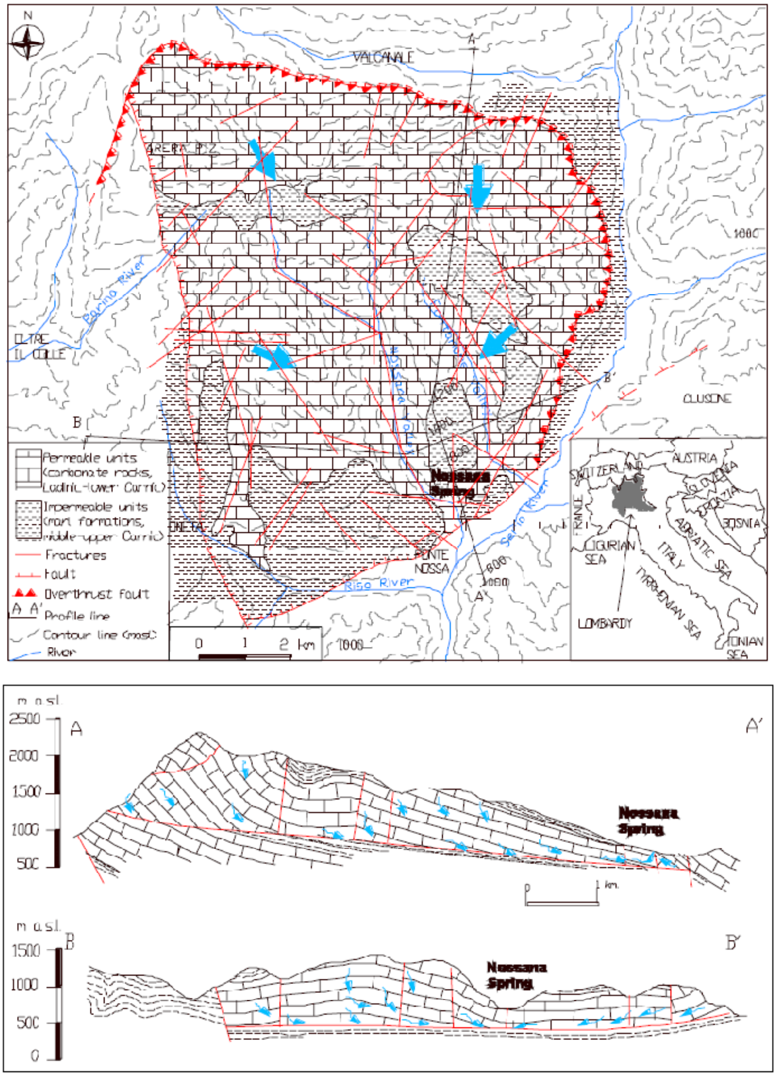

Figure 4.7. Location (box in the lower right corner), hydrogeological map and cross-sections of the catchments area of the Nossana Spring. The arrows both in plain and in the cross-section views show the main groundwater flow direction.

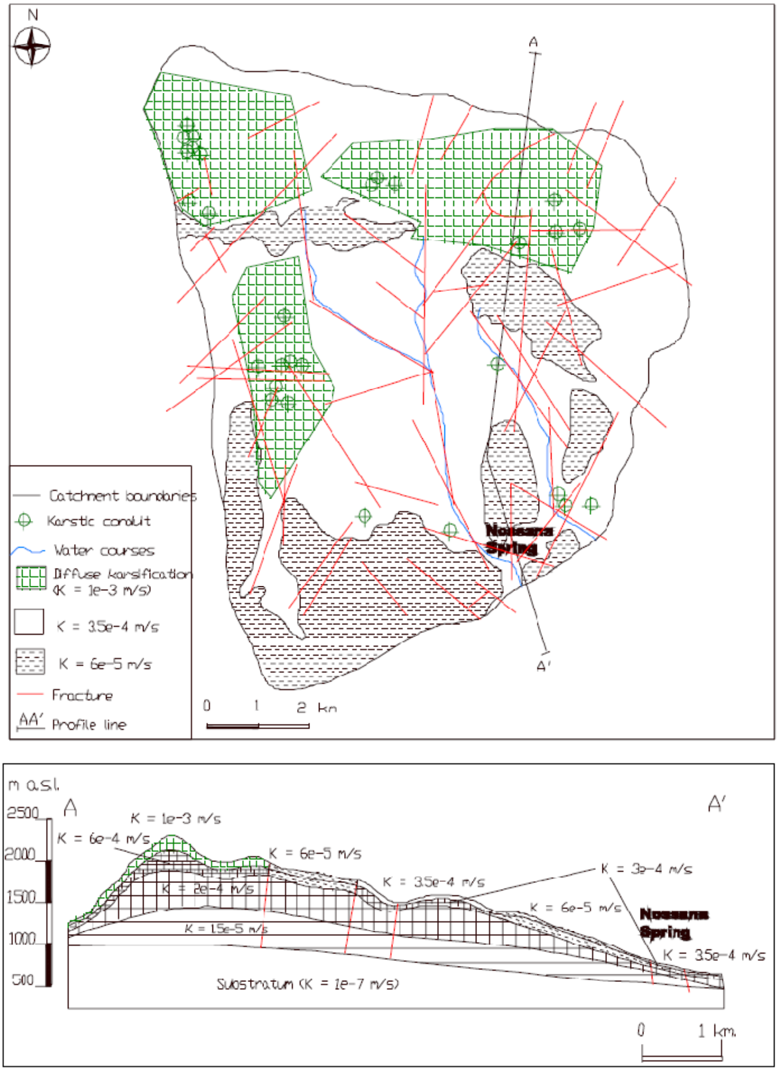

Figure 4.8. Conceptual model of the case study. In plain: the catchment boundaries, the surface waters (rivers and spring), the karstic evidences and fractures, the surface hydraulic conductivity map. In the cross-section: the 5 layers into which the domain was split in depth and the respective hydraulic conductivity values.

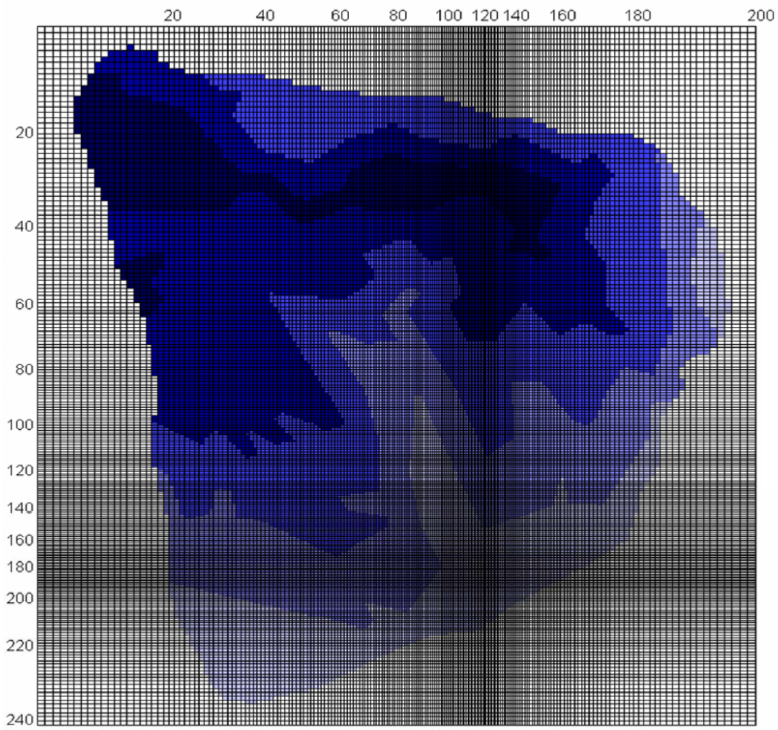

Altitude band (m a.s.l.)	Seasanal average recharge (mm)			
	Winter	Spring	Summer	Autumn
< 800 m a.s.l.	275	414	349	435
800-1200 m a.s.l.	236	380	350	398
1200-1600 m a.s.l.	119	278	352	289
1600-2000 m a.s.l.	80	245	352	253
> 2000 m a.s.l.	41	211	353	216

Figure 4.9. A plan view of the mesh used for the domain discretisation. The colours show the different recharge zones, corresponding to different altitude bands from below 800 m a.s.l. (the lightest colour) to above 2000 m a.s.l. (the deepest colour).

The trend of the hydraulic conductivity with the depth depends on a number of factors and, especially for a karst aquifer, it has to be calibrated whenever a specific case is studied. As for the Nossana Spring there are no data concerning the underground hydrogeological parameters, the hydraulic conductivity was supposed to be decreasing from the surface to the depth (Fig. 4.8). The decreasing rate was numerically calibrated later on.

The conceptual model was solved using the numerical model MODFLOW (Harbaugh et al., 2000). For a large flow scenario such as the present study, treatment of a fractured-karst medium as homogeneous might lead to a reasonably good agreement with an equivalent porous medium, due to the following reasons:

- the work scale can be considered a "very large field" (Bear and Berkowitz 1987), so that the water flow occurs inside a fractured porous medium that can be assimilated to a continuum;
- at this work scale, the fracture/conduit systems supplying the spring are fairly uniform and well interconnected (Croci et al., 2003);
- previous Authors demonstrated that the distributed parameter approach of the equivalent porous media can be successfully used to simulate large scale groundwater flow in a fractured-karstified aquifer, especially when the objective of the model is to simulate spring discharge (Scanlon et al., 2003), and having only data on spring discharge for the model calibration (Angelini and Dragoni, 1997).

The domain was split into 240x200 square cells with sizes having an average value equal to 50 m, ranging from 100 m in the external zone to 20 m along the main fracture/karst conduit of the Nossana Valley (Fig. 4.8). To simulate the decreasing permeability in depth, 5 layers having different thickness (Fig. 4.8) were considered. According to the geological setting of the area (Fig. 4.7), a low permeability substratum was simulated by introducing a base layer having hydraulic conductivity equal to 1e-7 m/s. The domain discretisation brings about a volume of the cells ranging from 1.2E4 m^3 for the first layer to 1E6 m^3 in depth. These volumes can be considered higher than the Representative Elementary Volume (Bear, 1972), generally ranging from 10^3 m^3 for the fractured superficial rock mass and 10^6 m^3 for the karstic aquifer (Civita, 2005). As far as boundary conditions are concerned, the following conditions were applied:

- no flow outside the catchment boundaries,
- river along the streams,
- drain for the Nossana spring.

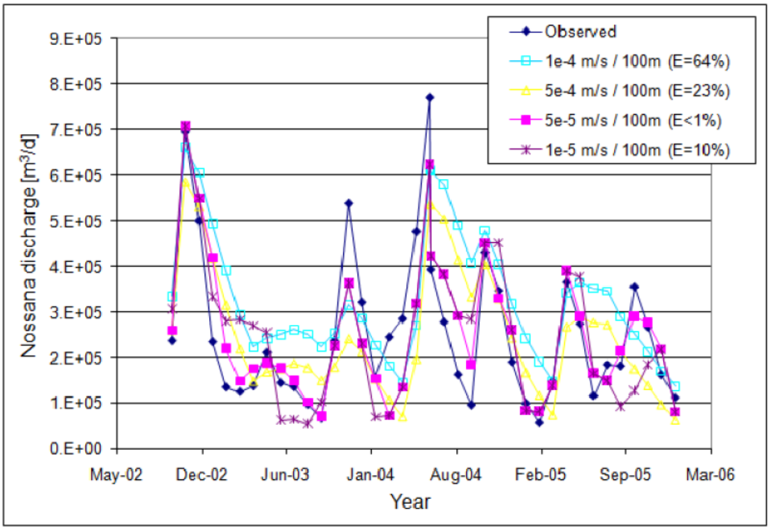

Figure 4.10. Comparison between the observed discharge of the Nossana Spring and the discharges simulated with different decreasing rates of the hydraulic conductivity with depth. For each simulation, the corresponding percent error between the simulated discharges and the observed ones are shown.

The rate of the hydraulic conductivity decreasing with depth was calibrated in order to simulate the discharge values measured in the Nossana Spring. As stated before, the only useful data for the model calibration was the spring discharge (corresponding to a single flow target point), whereas no head targets were available for the study area. Therefore, since no calibration statistics could be reconstructed, the model calibration was carried out with a trial and error technique at first in steady state, and then in transient-state, varying the in depth decreasing rate of the hydraulic conductivity (Fig. 4.10). During the calibration, both exponential and linear decreases were considered, obtaining that a linear decrease best fits the observed spring discharge in the specific case under exam. For each simulation, the percent error of the simulated discharges was calculated with respect to the observed ones (the corresponding values are shown in Figure 4.10) in order to obtain a good agreement with the observed Nossana discharge. As shown in the graph of Figure 4.9, despite the large complexity of the natural system, the model agreed with the historical flow data, with an average error equal to 1% considering a decreasing rate equal to 5E-5 m/s every 100 m of depth. Since there are no data on the hydraulic head of the aquifer, which is only known at the elevation of the spring, no further calibration of parameters was possible. In spite of that, the model seems to capture the salient features of the groundwater flow system, since the simulated head distribution is totally reasonable when compared with the topographic changes of the domain.

4.3. Example of Discrete Modeling Approach: Tunnel Inflow Assessment

As stated before, the application of discrete flow models is generally limited to simplified or limited cases or it is referred to very specific and detailed studies, such as tunnel inflow assessment. Groundwater inflow assessment is actually essential for the design of the tunnel drainage systems, as well as for the estimation of the environmental impact of drainage. When tunnels are drilled in fractured rock masses, the difficulties to forecast the water inflow location or the drainage processes increases, because the hydraulic behavior is neither homogeneous nor isotropic and the water flow is controlled by joints features (i.e. aperture, filling, roughness), joints dip and dip directions, fracturing degree (i.e. joint spacing, frequency and persistence, RQD, Rock Unit Volume; Scesi and Gattinoni 2009; Scesi and Gattinoni 2007; Lee and Farmer 1993; Min et al. 2004; Snow 1969; Louis 1974), discontinuities connectivity (Long and Witherspoon 1985; Rouleau and Gale 1985; Meyer and Einstein 2002), and by the lithostatic load (also depending on the tunnel depth), which can bring about great changes of the joints aperture (Bandis et al. 1983; Bai et al. 1999; Liu et al. 2000). The use of analytical solutions (Harr 1962; Goodman et al. 1965; Knutsson et al. 1996; Lei 1999; Kawecki 2000; Ribacchi et al. 2002; Cesano et al. 2003; El Tani 2003; Perrochet and Dematteis 2007; Hwang et al. 2007; Park et al. 2008) plays an important role in the first and quick estimation of tunnel inflow. Yet, the analytical formulas are generally valid for homogeneous and isotropic aquifer. On the contrary, rock masses are typically anisotropic and heterogeneous media, for which the traditional analytical solutions do not predict accurately tunnel drainage (Zhang and Franklin 1993; Fernandez and Moon 2010). Therefore, numerical simulations can help to analyse more complicated scenarios (Dunning et al. 2004; Molinero et al. 2002; Hwang and Lu 2007; Zangerl et al 2008a). Another alternative consists in integrating the two approaches (analytical and numerical) with the aim of modifying the traditional analytical methods for properly taking into account the rock mass complexity, as recently done by Moon and Fernandez (2009), that provides an analytical method for estimating groundwater inflow rate taking into account the groundwater table drawdown, and by Gattinoni and Scesi (2010), who pointed out an empirical relation in which tunnel inflow depends on geo-structural parameters of the rock mass.

In the following the example of a small diameter tunnel (Bergamo District, northern Italy), located at a medium depth, and realized within sedimentary rocks (mainly flysch of the Lombardy Series), characterized by a medium-low hydraulic conductivity, was analyzed (Figure 4.11). The tunnel, without waterproofing, developed below the water table for a length of 5.5 km. The tunnel was divided into eighth hydrogeological and geo-structural homogeneous stretches (Figure 4.11). For each one the hydraulic conductivity tensor and the corresponding equivalent hydraulic conductivity, relative to saturated rock mass, were calculated based on the geo-structural survey. Integrating this information with the results of pumping tests, it was also possible to consider the decreasing of permeability with depth. The hydraulic conductivity ellipses (Figure 4.11), in the vertical planes orthogonal to the tunnel direction, show a considerable medium anisotropy, in particular, in the stretches 2, 4 and 6, the main component of the hydraulic conductivity is almost vertical. For each homogeneous stretch a discrete model with the UDEC code was carried out.

In the modelling the joints stiffness values are considered independent from the effective normal stress, as the research was mainly oriented to study middle depth tunnel (at an average depth equal to 50 m corresponding to an average normal effective stress in the order of 1.5 MPa). However, the joints stiffness values were considered high enough to preclude differential joint displacement between blocks, that could bring about a local joint closure and a consequent uncontrolled rock bridge formation (Zangerl et al. 2008b).

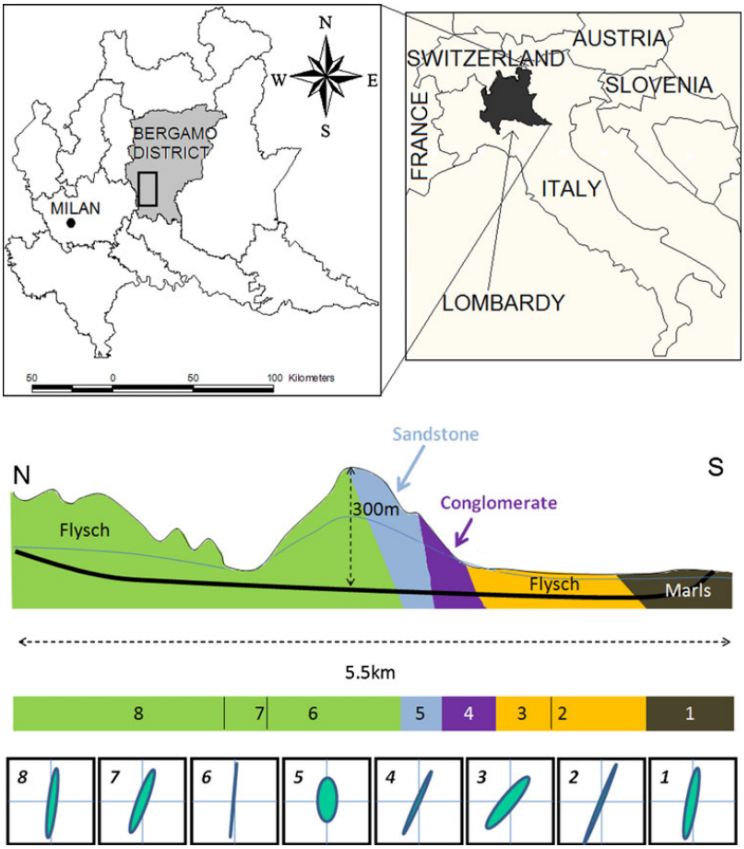

Figure 4.11. Geological cross section along the tunnel (shown as the dark line) in Bergamo District, northern Italy. The blue line is the water table. The numbers 1–8 indicate the homogeneous stretches in which the tunnel was divided, for which the hydraulic conductivity ellipses (in the plane orthogonal to the tunnel axes) are shown.

In the numerical modelling the following boundary conditions were applied:

- impermeable boundary along the bottom and along the same border of the tunnel location (right vertical boundary);
- constant load on the opposite side as regards the tunnel location (left vertical boundary);

- no displacements on the bottom and along the groundwater supply boundary;
- free hydraulic boundary conditions at the upper boundary of the modeling domain, simulating dry weather conditions.

The following initial conditions were considered:

- lithostatic load with lateral (horizontal) pressure coefficient equal to 0.5;
- hydrostatic load depending on the applied constant head boundary condition and complete saturation below water table.

The numerical simulations were carried out though a fully hydraulic-mechanical coupled approach. No flow boundary condition was applied to the tunnel, but the pore pressure (and the total radial stress too) along the tunnel is reduced to zero by the tunnel opening. This perturbation induces a drainage process into the discrete network fractures around the tunnel, bringing about a water table drawdown, which is determined only from pore pressure.

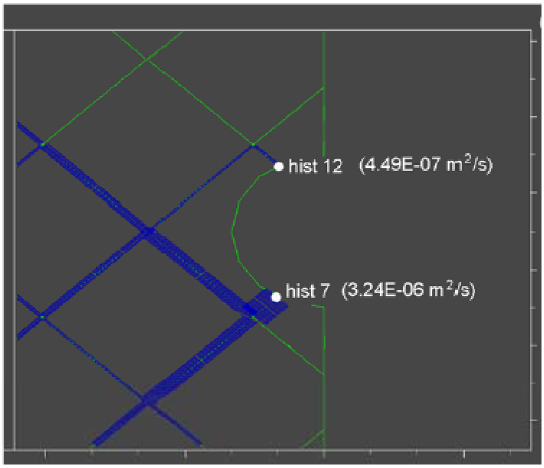

Figure 4.12. Example of model output. Water flow along joints is shown in blue (the line thickness corresponds to the flow rate), with the corresponding flow rate (named hist 7 and hist 12).

During the modelling, both the tunnel pre and post-excavation conditions were simulated until the steady-state condition was reached. At the end of each simulation groundwater tunnel inflow (Fig. 4.12) and water table drawdown along the tunnel axis (Fig. 4.13) were obtained.

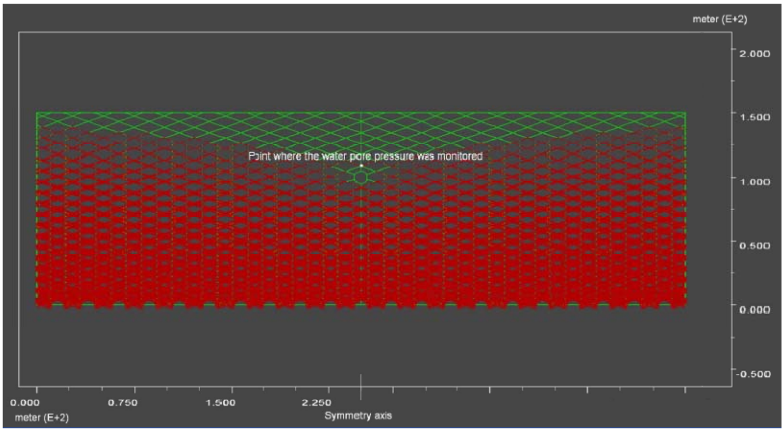

Figure 4.13. Example of the water pressures (in red) in post-excavation steady state.

The simulation results obtained by discrete approach were compared with results of different approaches:

- traditional analytic equations (in particular Goodman's and Ribacchi's equations), in which the tunnel inflow assessment is based on the equivalent hydraulic conductivity of the rock mass;
- 3D continuum groundwater flow modelling, in which the tensor of hydraulic conductivity is considered, assimilating the rock mass to an anisotropic and heterogeneous continuum;
- the empirical equation by Gattinoni and Scesi (2010), which through a correction of the Goodman equation accounts for geostructural parameters of the rock mass such as joint orientation, aperture, spacing and persistence.

The results obtained with the different approaches were then compared with the tunnel monitoring data, arising from the flow rate measured in the tunnel channel at different tunnel distances. These monitoring data allowed to calculate the tunnel inflow in the different stretches as the difference between the channel flow rate in the upstream and downstream sections.

The results comparison (Fig. 4.14) showed that the Goodman's equation provides highly overestimated values of the tunnel water inflow, especially in that sections where the rock mass anisotropy is higher, with maximum hydraulic conductivity in the direction close to the vertical. This overestimation can be corrected by using the Ribacchi's equation, through the introduction of the hydraulic conductivity of the lining. Yet, as results, the best estimation can be obtained by using the empirical relation by Gattinoni and Scesi (2010), which provides values comparable to those obtained by discrete numerical modelling and actually observed in the tunnel (Fig. 4.14). These results confirm the importance of considering the discontinuous nature of the medium, with particular reference to its structural setting.

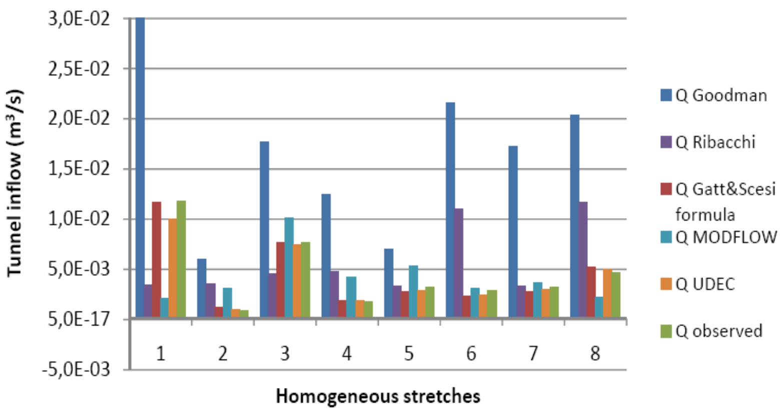

Figure 4.14. Comparison between tunnel inflow obtained through different approaches.

REFERENCES

Alboin, C., Jaffre, J., Joly, P., Roberts, J., Serres, C. (2002), «A comparison of methods for calculating the matrix block source term in a double porosity model for contaminant transport», *Comput. Geosci*., 6, pp. 523-543.

Andersson, J., Dverstorp, B. (1987), «Conditional simulations of fluid flow in three-dimensional network of discrete fractures», *Water Resources Res*., 23, pp. 1876-1886.

Angelini P., Dragoni W. (1997), «The problem of modelling limestone springs: the case of Bagnara (North Apennines, Italy) », *Ground Water* 35(4):612-618.

Bai, M., Elsworth, D., Roegiers, J.C. (1997), «Triple-porosity analysis of solute transport», *J. Contam. Hydro*, 28, pp. 247-266.

Bai, M., Meng, F., Elsworth, D., Roegiers, J.C. (1999), «Analysis of stress-dependent permeability in non orthogonal flow and deformation fields», *Rock Mech. Rock Eng*., 32 (3), pp. 195-219.

Bandis, S.C., Barton, N.R., Christianson, M. (1985), «Application of a new numerical model of joint behaviour to rock mechanics problems», *Fundamentals of Rock Joints. Proceedings of the International Symposium on Fundamentals of Rock Joints*, Bjorkliden, September 1985, Luleå, Sweden: Centek, pp. 345-356.

Barenblatt, G.E., Zheltov, I.P., Kochina, I.N. (1960), «Basic concepts in the theory of seepage of homogeneous fluids in fissured rocks», *J. Appl. Math. and Mech.*, 24, pp. 1286–1303.

Bear, J. (1972), «Dynamics of Fluids in Porous Media», Elsevier, New York.

Bear, J. (1993), «Modelling flow and contaminant transport in fractured rocks», in J. Bear, C.F. Tsang, G. DeMarsily (eds), *Flow and Contaminant Transport in Fractured Rock*, Academic Press, San Diego (California), pp. 1-10.

Bear, J., Berkowitz, B. (1987), «Groundwater flow and pollution in fractured rock aquifers», in P. Nowak (a cura di), *Development in Hydraulic Engineering*, vol. 4, Elsevier, New York.

Bini A., Forcella F., Jadoul F., Orombelli G. (2000), (edited by) *Carta Geologica della Provincia di Bergamo alla scala di 1:50000.*

Brace, W.F. (1980), «Permeability of argillaceous and crystalline rocks», *Int. J. Rock Mech. Min. Sci. & Geomech. Abstr.*, 17, pp. 241-251.

Cacas, M.C., Ledoux, E., DeMarsily, G., Tillie, B., Barbreau, A., Durand, E., Feuga, B., Peaudecerf, P. (1990), «Modelling fracture flow with a stochastic discrete fracture network: calibration and validation 1. The flow model», *Water Resources Res.*, 26, pp. 479-789.

Cesano D, Bagtzoglou AC, Olofsson B (2003), «Quantifying fractured rock hydraulic heterogeneity and groundwater inflow prediction in underground excavations: the heterogeneity index». *Tunn Undergr Space Technol* 18:19–34

Chardon M. (1975), «*Les Prealpes Lombardes et leurs bordures*», These Univo Aix-Marseille.

Civita, M. (2005), «*Idrogeologia applicata e ambientale*», Casa Editrice Ambrosiana, Milano.

Clifford K. Ho (2001), «Dual porosity vs. dual permeabilità models of matrix diffusion in fractured rock», Sandia National Laboratories. Albuquerque, NM (USA).

Croci A., Francani V., Gattinoni P. (2003), «Studio idrogeologico del bacino del Torrente Esino», *Quaderni di geologia applicata*, 10 (2): 148-166.

Dershowitz, W.S., Einstein, H.H. (1988), «Characterizing rock joint geometry with joint system models», *Rock Mech. Rock Eng.*, 21 (1), pp. 21-51.

Dietrich P., Helmig R., Sauter M., Hotzl H., Kongeter J., Teutsch G. (eds) (2005), «*Flow and transport in fractured porous media*», Springer.

Diodato, D.M. (1994), «A Compendium of Fracture Flow Codes», Energy System Division, Argonne National Laboratory, Technical Memorandum 96.

Dunning, C.P., Feinstein, D.T., Hunt, R.J., Krohelski, J.T. (2004), «Simulation of ground-water flow, surface-water flow, and a deep sewer tunnel system in the Menomonee Valley, Milwaukee, Wisconsin», *USGS Scientific Investigations Report* 2004, 5031.

Dverstorp, B., Andersson, J. (1989), «Application of the discrete fracture network concept with field data: possibilities of model calibration and validation», *Water Resources Res*., 25 (3), pp. 540-550.

El Tani M (2003), «Circular tunnel in a semi-infinite aquifer», *Tunn Undergr Space Technol* 18:49–55

Fernandez G, Moon J (2010), «Excavation-induced hydraulic conductivity reduction around a tunnel, part 1: guideline for estimate of ground water inflow rate», *Tunn Undergr Space Techn.* doi:10.1016/j.tust.2010.03.006

Gattinoni P., Scesi L. (2010), «An empirical equation for tunnel inflow assessment: the application to a case history in sedimentary rock masses». *Hydrogeology Journal*. Springer. DOI: 10.1007/s10040-010-0674-1

Goodman, R.E., Moye, D.G., Van Schalkwyk, A., Javandel, I. (1965), «Ground water inflow during tunnel driving», *Eng. Geol*., 2, pp. 39-56.

Harbaugh AW, Banta ER, Hill MC, McDonald MG (2000), *MODFLOW-2000, the U.S. Geological Survey modular ground-water model—user guide to modularization concepts and the ground-water flow process*. U.S. Geological Survey open-file report 00-92, 121 pp.

Harr ME (1962), «*Groundwater and seepage*», McGraw-Hill, New York, pp 249–264

Hsieh P.A. (1998), «Scale effects in fluid flow through fractured geologic media», In: Sposito G. (ed.) *Scale Dependence and Scale Invariance in Hydrology*. Cambridge University Press, Cambridge, UK, 335–353.

Hung, C., Evans, D.D. (1985), «A 3-dimensional computer model to simulate fluid flow and contaminant transport through a rock fracture system», NUREG/CR-4042, US Nuclear Regulatory Commission.

Huyakorn, P.S., Lester, B.H., Faust C.R. (1983), «Finite element techniques for modeling groundwater flow in fractured aquifers», *Water Resources Res.*, 19 (4), pp. 1019-1035.

Hwang JH, Lu CC (2007), «A semi-analytical method for analyzing the tunnel water inflow», *Tunn Undergr Space Technol* 22(1):39–46

Itasca (1999), «*UDEC, User's guide*», Itasca Consulting Group Inc., Minneapolis.

Jadoul F., Pozzi R., Pestrin S. (1985) «La sorgente Nossana: inquadramento geologico e idrologico», *Riv. Mus. Sc. Nat.* BG, 9: 129-140.

Jeong, W.C., Bruel, D., Hicks, T. (1999), «Modelling the influence of fault zone heterogeneity on groundwater flow and radionuclide transport», *Proc. of Eurowaste '99, 5th European Commission Conference on Radioactive Waste Management and Disposal and Decommissioning*.

Kawecki, M.W. (2000), «Transient flow to a horizontal water well», *Ground Water*, 38/6, pp. 842-850.

Kazemi, H. (1969), «Pressure transient analysis of naturally fractured reservoirs with uniform fracture distribution», *Soc. Pet. Eng. J.*, 9, pp. 451-462.

Kendorski, F.S., Mahtab, M.A. (1976), «Fracture patterns and anisotropy of San Manuel Quartz Monzanite», *Bull. Assoc. Eng. Geol.*, 13, pp. 23-31.

Knutsson, G., Olofsson, B., Cesano, D. (1996), «Prognosis of groundwater inflows and drawdown due to the construction of rock tunnels in heterogeneous media», *Res. Proj. Rep. Kungl. Tekniska*, Stockholm.

Kraemer, S.R., Haitjema, H.M. (1989), «Regional modelling of fractured rock aquifers», in G. Jousma et al. (eds), *Groundwater Contamination: Use of Models in Decision-Making*, Kluwer Academic Publishers, Dordrecht, pp. 467-476.

La Pointe, P.L., Wallmann, P.C., Follin, S. (1996), «Continuum modelling of fractured rock masses: is it usefull?», in G. Barla (a cura di), *Eurock 96*, Balkema, Rotterdam, pp. 343-350.

Lee C.H., Farmer I (1993), «*Fluid flow in discontinuous rocks*», Chapman&Hall, New York.

Lei, S., (1999), «An analytical solution for steady flow into a tunnel», *Ground Water*, 37 (1), pp. 23-26.

Liu, J., Elsworth, D., Brady, B.H., Muhlhaus, H.B. (2000), «Strain-dependent fluid flow defined through rock mass classification schemes», *Rock Mech. Rock Eng.,* 33 (2), pp. 75-92.

Long, J.C.S., Witherspoon, P.A. (1985), «The relationship of the degree of interconnaction to permeability of fracture networks», *J. Geophys. Res.*, 90 (B4), pp. 3087-3098.

Louis, C. (1974), «Introduction à l'hydraulique des roches», *Bur. Rech. Geol. Min.*, 4/3, pp. 283-356.

Machado, L.I., Silva, F., Duias, R., Laiginhas, C. (2001), «GIS Technologies Applied to Modelling Fluid Circulation in Carbonate Massifs – The Estremos Anticline (Portugal) », *Geospatial World*, Atlanta.

Manev, G., Avramova-Tacheva, E. (1970), «On the valuation of strenght and resistance condition of the rocks in natural rock massif», *Proc. 2nd Cong. Int. Soc. Rock. Mech*., Belgrade, Paper 1-10, pp. 59-64.

McCaffrey, M.A., Adinolfi, A.M. (2003), «Evaluating groundwater behavior in jointed rock subject to dewatering», *39th U.S. Rock Mech. Symp*.

Meyer, T., Einstein, H.H. (2002), «Geologic stochastic modeling and connectivity assessment of fracture systems in the Boston Area», *Rock Mech. Rock Eng.*, 35 (1), pp. 23-44.

Min, K.B., Jing, L., Stephansson, O. (2004), «Determining the equivalent permeability tensor for fractured rock masses using a stochastic REV approach: method and application to the field data from Sellafield, UK», *Hydrogeology Journal*, 12 (5), pp. 497-510.

Molinero, J., Samper, J., Juanes, R. (2002), «Numerical modelling of the transient hydrogeological response produced by tunnel construction in fractured bedrocks», *Engineering Geology*, 64, pp. 369-386.

Moon J, Fernandez G (2009), « Effect of excavation-induced groundwater level drawdown on tunnel inflow in a jointed rock mass» *Eng Geol* 110(3–4):33–42

Moutsopoulos, K.N., Konstantinidis, A.A., Meladiotis, I.D., Tzimopoulos, C.D., Aifantis, E.C. (2001), «Hydraulic and contaminant transport in multiple porosity media», *Transport Porous Media*, 42, pp. 265-292.

Nastev M., Morin R., Gordin R., Rouleau A. (2008), «Developing conceptual hydrogeological model for Potsdam sandstones in southwestern Quebec, Canada», *Hydrogeology Journal* 16: 373-388.

Oxtobee, J.P.A., Novakowski, K.S. (2003), «Ground water/surface water interaction in a fractured rock aquifer», *Ground Water*.

Papini, M., Scesi, L., Bianchi, B. (1994), «Studi finalizzati alla previsione delle venute d'acqua in galleria», *Costruzioni*.

Park KH, Owatsiriwong A, Lee GG (2008), «Analytical solution for steady-state groundwater inflow into a drained circular tunnel in a semi-infinite aquifer: a revisit», *Tunn Undergr Space Technol* 23:206–209

Perrochet P, Dematteis A (2007): «Modeling transient discharge into a tunnel drilled in heterogeneous formation» *Ground Water* 45(6):786–790

Rasmussen, T.C. (1988), *«Fluid flow and solute transport through three-dimensional networks of variably saturated discrete fractures»*, Ph.D. Dissertation, Department of Hydrology and Water Resoucerces, University of Arizona.

Raven K.G., Gale, J.E. (1976), «Evaluation of structural and groundwater conditions in underground mines and excavations: subsurface containment of solid radioactive wastes», *Geol. Survey of Canada*, Progress Report. EMR/JSC-RW.

Ribacchi, R. Graziani, A., Boldini, D. (2002), «Previsione degli afflussi d'acqua in galleria e influenza sull'ambiente», *Meccanica e Ingegneria delle rocce*, MIR, Torino, pp. 143-199.

Robinson, P.C. (1982), «Connectivity of fracture system – A percolation theory approach», Theoretical Physics Division, AERE Arwell, DOE report no. DOE/RW/81.028.

Rouleau, A., Gale, J.E. (1985), «Statistical characterisation of the fracture system in the Stripa Granite, Sweden», *Int. J. Rock Mech. Min Sci. & Geomech. Abstr.*, 22, pp. 353-367.

Rowe, R.K., Booker, J.R. (1990), «Contaminant migration in a regular two or three dimensional fractured network: reactive contaminants», *International Journal of Numerical and Analytical Methods in Geomechanics*, 14, pp. 401-425.

Samardzioska, T., Popov, V. (2005), «Numerical comparison of the equivalent continuum, non homogeneous and dual porosity models for flow and transport in fractured porous media», *Advances in Water Resources*, 28 (3), pp. 235-255.

Scanlon B.R., Mace R.E., Barret M.E., Smith B. (2003) «Can we simulate regional groundwater flow in a karst system using equivalent porous media models? Case study, Barton Springs Edwards aquifer, USA», *Journal of Hydrology* 276:137-158.

Scesi L., Gattinoni P. (2009): “*Water Circulation in Rocks*” Springer, ISBN: 978-90-481-2416-9, pp. 1-165.

Scesi L., Gattinoni P. (2007): “Roughness control on hydraulic conductivity in fractured rocks” *Hydrogeology Journal*. Springer-Berlin. Heidelberg. N. 15, pp. 201-211.

Snow, D.T. (1969), «Anisotropic permeability of fractured media», *Water Resources Res.*, 5.

Sudicky, E.A. (1990), «The Laplace transform Galerkin technique for efficient time-continuous solution of solute transport in double-porosity media», *Geoderma*, 46, pp. 209–232.

Warren, J.E., Root, P.J. (1963), «The behavior of naturally fractured reservoirs», *Soc. Pet. Eng. J. Trans. ASME* 228, pp. 245-255.

Zangerl C, Eberhardt E, Evans KF, Loew S (2008a), «Consolidation settlements above deep tunnels in fractured crystalline rock: part 2, numerical analysis of the Gotthard highway tunnel case study», *Int J Rock Mech Min Sci* 45 (2008):1211–1225.

Zangerl C, Evans KF, Eberhardt E, Loew S (2008b), «Normal stiffness of fractures in granitic rock: a compilation of laboratory and in-situ experiments», *Int J Rock Mech Min Sci* 45(2008):1500–1507.

Zhang L, Franklin JA (1993), «Prediction of water flow into rock tunnels: an analytical solution assuming a hydraulic conductivity gradient», *Int J Rock Mech Min Sci* 30:37–46.

INDEX

A

algorithm, 26
anisotropy, 3, 38, 42, 46
aquifers, vii, 3, 44, 46
assessment, 37, 41, 45, 47

B

base, 35
bonds, 14

C

calibration, 24, 35, 36, 44, 45
case study, 23, 33, 49
catchments, 32
circulation, vii, 1, 4
classification, 47
closure, 26, 38
color, iv
compilation, 49
complexity, 28, 37, 38
composition, 4
computer, 45
conceptual model, vii, 2, 3, 6, 7, 8, 9, 23, 35
conductivity, 5, 8, 11, 12, 13, 14, 22, 24, 26, 28, 30, 31, 33, 34, 35, 36, 38, 39, 41, 42, 45, 49
Congress, iv
connectivity, 5, 37, 47
consolidation, 1
constant load, 39
construction, 3, 46, 47
contaminant, 29, 43, 44, 45, 47
cooling, 1
copyright, iv
cracks, 1
crystalline, 44, 49
crystals, 1

D

damages, iv
data availability, 6, 9
deformation, 26, 43
depth, 5, 7, 11, 31, 33, 34, 35, 36, 37, 38
diffusion, 44
discharges, 36
discontinuity, 4, 7, 11, 12, 13, 14, 16, 17, 18, 21, 23, 24, 28, 30
dispersion, 29
displacement, 26, 38
distribution, 2, 4, 9, 24, 27, 37, 46
DOI, 45

drainage, 37, 40
drawing, 27
dynamic loads, 25

E

elaboration, 5, 24
electric circuits, 25
engineering, vii
environmental impact, 37
European Commission, 46
evapotranspiration, 31
excavations, 44, 48
exchange rate, 30

F

families, 7, 14, 16, 17, 18
fluid, 14, 28, 43, 45, 47
formation, 5, 31, 38, 48
formula, 31
fractures, 1, 3, 5, 7, 9, 14, 22, 24, 26, 28, 29, 30, 31, 33, 40, 43, 48, 49
fragments, 1

G

geometry, 29, 30, 44
granules, 1
graph, 37
gravity, 11
groundwater, vii, 3, 5, 18, 21, 22, 23, 24, 25, 30, 31, 32, 35, 37, 38, 40, 41, 44, 46, 47, 48

H

height, 4
heterogeneity, 3, 27, 44, 46
history, 45
humidity, 18
hypothesis, 25

I

identification, vii, 2
influenza, 48
injury, iv
interface, 29, 30
Italy, 15, 31, 38, 39, 43

J

joints, 3, 4, 5, 6, 7, 9, 11, 26, 29, 37, 38, 40

L

laws, 8, 25
lead, 35
light, 18, 29
limestone, 43

M

magnitude, 31
mass, 1, 3, 4, 5, 6, 7, 8, 11, 14, 21, 22, 25, 35, 38, 41, 42, 47
matrix, 9, 29, 30, 43, 44
matter, iv
mechanical properties, 26
media, 11, 25, 28, 30, 38, 45, 46, 47, 49
migration, 48
Minneapolis, 46
modelling, 8, 23, 38, 39, 41, 42, 43, 46, 47
models, 23, 24, 27, 28, 29, 30, 37, 44, 48, 49
modulus, 13
moisture, 4
Moon, 38, 45, 47

N

numerical analysis, 49

O

one dimension, 29

P

percolation, 2, 11, 12, 13, 18, 48
percolation theory, 48
permeability, 1, 3, 4, 5, 7, 11, 18, 21, 26, 29, 35, 38, 43, 47, 49
permission, iv
pollution, 44
porosity, 1, 5, 7, 24, 28, 29, 30, 43, 44, 47, 48, 49
porous media, vii, 1, 24, 35, 44, 48, 49
Portugal, 47
precipitation, 31
preparation, iv
probability, 18
propagation, 29

Q

Quartz, 46

R

radioactive waste, 48
radius, 18
reality, 7
recommendations, iv
reconstruction, vii, 3, 22, 26
resistance, 47
response, 25, 29, 47
rights, iv
roughness, 4, 5, 37
Rouleau, 14, 37, 47, 48
rules, 5

S

saturation, 18, 24, 40
services, iv
settlements, 49
shape, 1
shear, 24, 25
showing, 2
simulation, 23, 25, 36, 41
simulations, 38, 40, 43
solution, vii, 27, 46, 48, 49
Spring, 30, 31, 32, 34, 36
stability, 3, 27
standard deviation, 26
state, 36, 41, 48
statistics, 36
stochastic model, 47
storage, 28, 29
stratification, 1
stress, 4, 26, 38, 40, 43
structure, 3, 5, 23
Sweden, 43, 48

T

talc, 15
target, 36
techniques, 25, 46
temperature, 31
transport, 43, 44, 45, 46, 47, 48, 49
transportation, 29
treatment, 35
trial, 36

U

U.S. Geological Survey, 45
UK, 45, 47
uniform, 35, 46
USA, 44, 49

V

validation, 44, 45
valuation, 47
variations, 4, 7

viscosity, 26

W

water, vii, 1, 2, 3, 4, 5, 7, 11, 14, 17, 18, 19, 21, 22, 25, 26, 28, 29, 31, 35, 37, 38, 39, 40, 41, 42, 45, 46, 48, 49
watertable, 12
Wisconsin, 45